Supporting Information for

Detailed Observation of Multiphoton Emission Enhancement from a Single Colloidal Quantum Dot Using a Silver-Coated AFM Tip

Hiroki Takata[‡], Hiroyuki Naiki[†], Li Wang[‡], Hideki Fujiwara[§], Keiji Sasaki[§], Naoto Tamai[‡], and Sadahiro Masuo[†]*

[‡]Department of Chemistry, Kwansei Gakuin University, 2-1 Gakuen, Sanda, Hyogo 669-1337, Japan

[†]Department of Applied Chemistry for Environment, Kwansei Gakuin University, 2-1 Gakuen, Sanda, Hyogo 669-1337, Japan

[§]Research Institute for Electronic Science, Hokkaido University, Sapporo, 001-0020 Japan

1. Instrument setup

The dependence of the emission behavior of the single NQD on the NQD-AgTip distance (*z*-distance) was measured using an inverted confocal microscope (Olympus, IX-71) combining with an AFM system (JPK Instruments, NanoWizard II) system reported elsewhere.[1] In this setup, an AFM was placed on the top of an inverted confocal microscope. In addition to the three closed-loop, piezo-driven axes of the AFM head, a two-axis, closed-loop, and piezo-driven sample stage was used. As an excitation light source, pulsed lasers oscillating at 405 nm and 465 nm (10.0 MHz, 90 ps FWHM; PicoQuant) were used. To produce the *z*-polarized excitation beam, the laser beam was linearly polarized by a Gran-Thomson polarizer and a λ/2 wave plate and then converted to a radially polarized beam by a radial polarization converter (ARCoptix). The excitation laser beam was reflected by a dichroic mirror (Semrock, Di02-R488) in the microscope and was then focused to a diffraction-limited spot on a sample by an objective lens (100×, NA 1.4; Olympus). The PL emission photons from the single NQD were collected by the same objective lens and passed through a confocal pinhole (100 μm) with long-pass (LP02-512RU, Semrock) and short-pass filters (Semrock, FF01-694/SP) to remove the excitation laser and the 800 nm laser of the AFM system, respectively. Subsequently, half of the photons were detected by a spectrometer (Acton Research Corporation, SpectraPro2358) equipped with a cooled CCD camera (Princeton Instruments, PIXIS400B). The remaining half of the photons passed through a band-pass filter (Semrock, FF01-607/36) that was suitable for the PL band of the isolated NQDs. Next, the photons were divided equally by a 50/50 nonpolarizing beam splitter cube into two beam paths and then detected by two avalanche single-photon counting modules (APD: PerkinElmer, SPCM-AQR-14). The signals from both APDs were connected to the router of a time-correlated single-photon counting (TCSPC) PC board (Becker & Hickl, SPC630) to measure the PL lifetime and to collect data for the photon correlation histogram. The signal from one of the two APDs was delayed using a delay generator (Stanford Research, DG535) to compensate for the dead time of the TCSPC board. Time-resolved data were acquired using a first-in-first-out mode, in which the arrival time after the beginning of the acquisition, the time delay

between the start and stop pulses, and the detection channel were registered for each detected PL photon. The data were analyzed using a homemade LabVIEW routine that allowed for the simultaneous measurement of PL intensity trajectory, PL lifetime, and the photon correlation histogram of single NQDs. The time-resolution of the lifetime measurement, i.e., the instrumental response function (IRF) of the system, was estimated by the deconvolution of the fluorescence decay curve of erythrosine in water, which has a reported fluorescence lifetime of 87 ps.[2] The estimated IRF was approximately 0.3 ns.

2. Scattering spectrum measurement of the AgTip

The scattering spectrum of the AgTip was measured by contacting the AgTip with the surface of a taper fiber coupled with a white-light source.[3] A tapered fiber (diameter ≈ 400 nm) was fabricated by heating a fused-silica single-mode optical fiber (Thorlabs, 780HP) with a ceramic heater while stretching both ends of the fiber. We monitored the transmittance in the tapered fibers at 780 nm during the fabrication process. The transmittances of the tapered fibers in the experiment were greater than 0.90.

A white-light source was introduced into the tapered fiber as a probe light. The approach of the AgTip and its contact with the surface of the tapered fiber were controlled using piezo manipulators (PI-Polytec, P- 621.1CD, P-621.ZCD). These components were placed in a plastic box to maintain stable conditions. The transmitted intensity spectrum of the incident white light from the end of the tapered fiber without the AgTip was measured by a spectrometer (JASCO Corporation; iDus; Andor). The scattered light from the AgTip was collected using a microscopy system positioned on the top of the AgTip. The scattering light was collected by an objective lens with 0.42 NA, and the scattered intensity spectrum at the AgTip was measured by the spectrometer. The scattering spectrum of the AgTip was then obtained from the scattered intensity spectrum at the AgTip divided by the transmitted white-light intensity spectrum.

3. Numerical simulation of the AgTip

Numerical simulations were conducted using finite element analysis (Optical Module, Comsol

Multiphysics 5.2) to correlate the experimental data of the AgTip with the predicted properties of extinction and field enhancement of a simplified AgTip in air. The dimensions and shape of the AgTip were determined from the SEM measurement of the AgTip. The optical and physical properties of Ag were based on the definition in the Comsol material library from the paper Johnson and Christy.[4] A plane wave was used as the excitation source, and E was parallel to the AgTip. We define the electric field enhancement factor as the ratio of the electric field intensity on the AgTip surface ($|\text{ewfd.norm}E|^2$) and light source ($|E_0|^2$).

The primary difficulty encountered in the simulation was the determination of the shape and effective length of the AgTip. Thus, the shape and the effective length were varied to reproduce the scattering spectrum of the AgTip. Initially, we assumed a cone-shaped AgTip with tip radius a = 30 nm and varied the tip length h. Figure S1(a-d) shows the distribution of the electric field enhancement of the cone-shaped AgTips with the h = 60, 120, 180, and 240 nm, and Figure S1(e) shows the simulated extinction spectra of the AgTips. In Figure S1(e), the peak wavelength red-shifted and the intensity increased as h increased. On the basis of these results, we reproduced the experimentally measured spectrum of the AgTip by assuming h=60 nm.

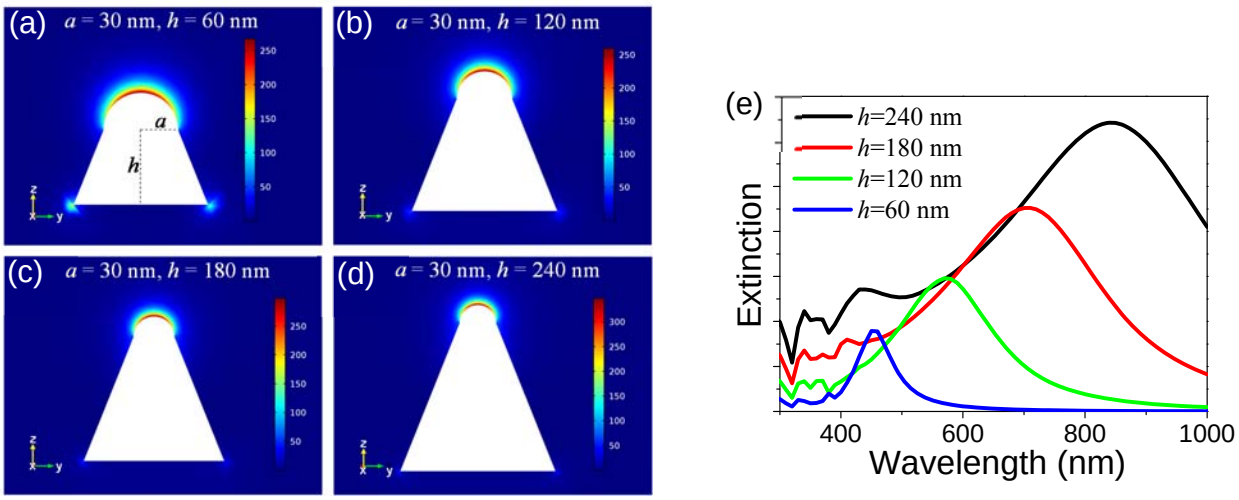

Figure S1. (a-d) Distributions of the electric field enhancement simulated by assuming a cone-shaped AgTip with a = 30 nm and different h: (a) h = 60 nm, (b) h = 120 nm, (c) h = 180 nm, and (d) h = 240 nm. (e) Simulated extinction spectra at the top of the AgTip assuming the cone-shaped AgTip shown in (a-d).

We next investigated the influence of the shape. We assumed a cone-shaped structure with a = 30 nm with the bottom radius (a_b) varied. Figure S2(a-c) shows the distribution of the electric field enhancement of the cone-shaped AgTips with a_b = 37 (a), 44 (b), and 54 nm (c), and Figure S2(d) shows the simulated extinction spectra at the top of the AgTips. In Figure S2(d), the peak wavelength slightly red-shifted, the intensity increased and the width of the spectra broadened with increasing a_b. The change of a_b in this range did not remarkably influence the experimentally obtained spectrum of the AgTip.

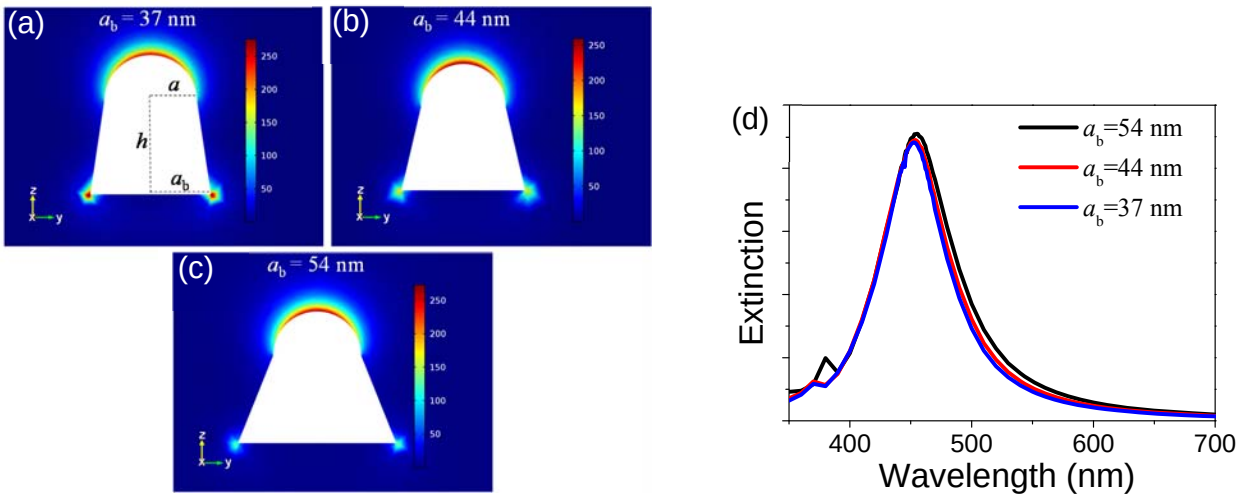

Figure S2. (a-c) Distributions of the electric field enhancement simulated by assuming a cone-shaped AgTip with a = 30 nm and different a_b; (a) a_b = 37 nm, (b) a_b = 44 nm, and (c) a_b = 54 nm. (d) Simulated extinction spectra at the top of the AgTip assuming the cone-shaped AgTip shown in (a-c).

4. Emission behavior of the single NQD with an approach of the AgTip

4-1. Excitation at 405 nm

Figures S3 and S4 show the two representative emission behaviors of a single NQD with an approach of the AgTip measured at 405 nm excitation. The PL intensity, PL lifetime, normalized amplitude, and the $g^{(2)}(0)$ value obtained from Figures S3 and S4 are summarized in Table S1. In both figures, the PL intensity decreased, the decay curves shortened, and the probability of multiphoton

emission increased with decreasing z-distance; after the AgTip was retracted, the emission behavior returned to the original emission behavior, similar to the emission behavior discussed in the main text.

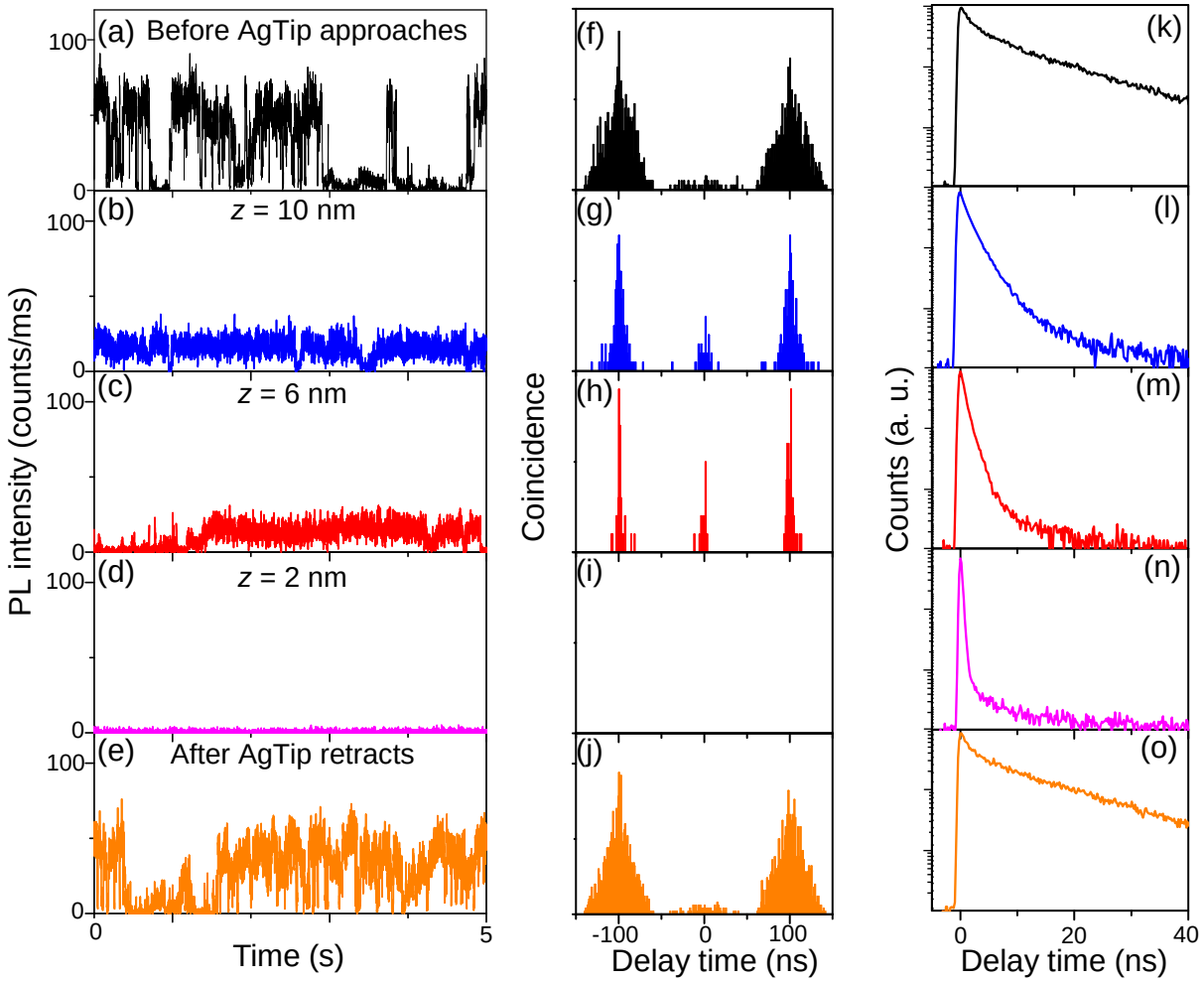

Figure S3. Time traces of the PL intensity (a-e), photon correlation histograms (f-j), and PL decay curves (k-o) detected from a single NQD depending on the *z*-distance at 405 nm excitation: (a, f, k) before the AgTip was advanced; (b, g, l) z=10 nm; (c, h, m) z=6 nm, (d, i, n) z=2 nm; and (e, j, o) after the AgTip was retracted.

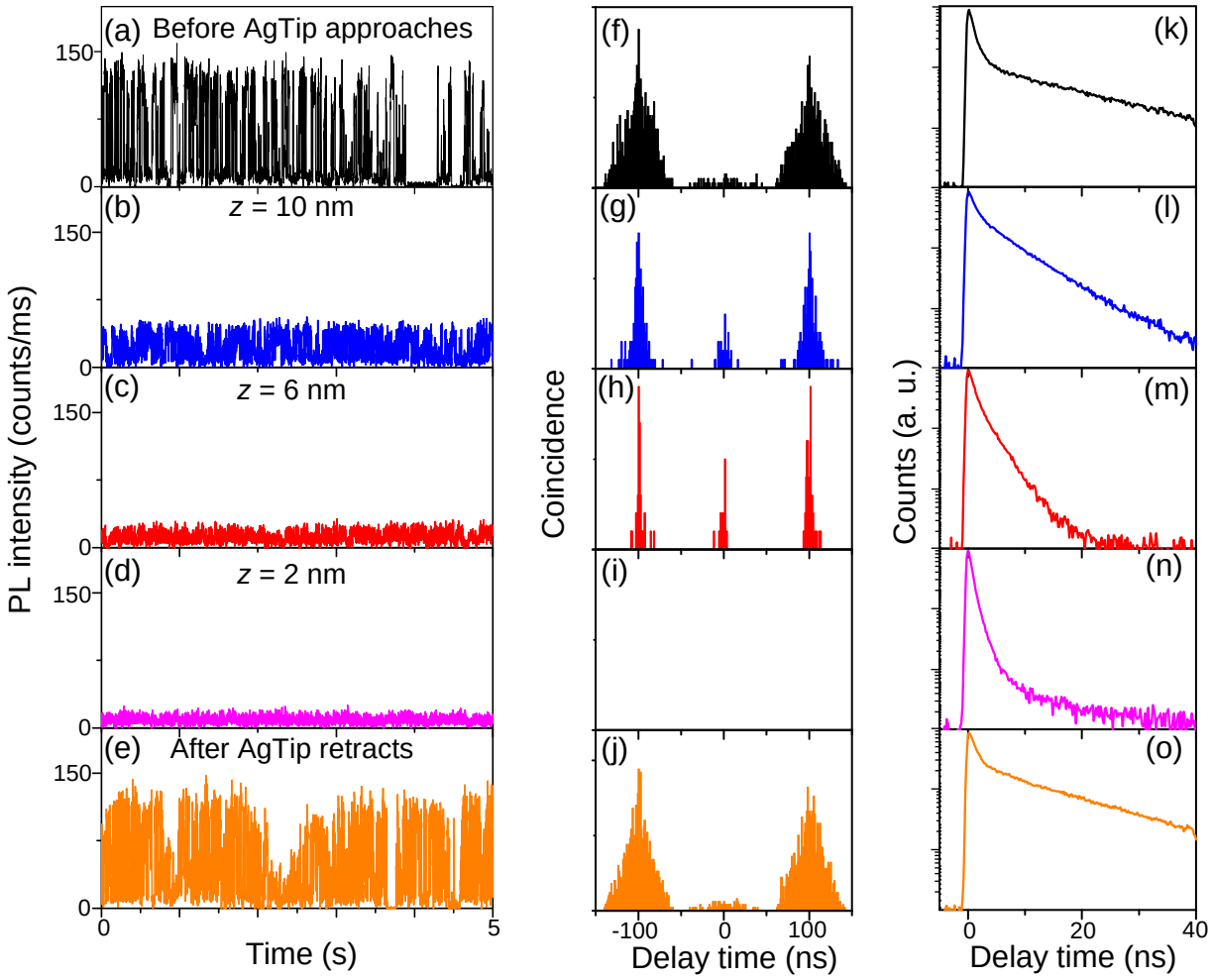

Figure S4. Time traces of the PL intensity (a-e), photon correlation histograms (f-j), and PL decay curves (k-o) detected from a single NQD depending on the *z*-distance at 405 nm excitation: (a, f, k) before the AgTip was advanced; (b, g, l) z = 10 nm; (c, h, m) z = 6 nm; (d, i, n) z = 2 nm; and (e, j, o) after the AgTip was retracted.

Table S1. The PL intensity, fitting parameters for the PL decay curves, and $g^{(2)}(0)$ obtained from the single NQDs shown in Figures S3 and S4.

	z-distance	Intensity (cts/ms)	τ_1 (ns)	α_1 (%)	τ_2 (ns)	α_2 (%)	τ_3 (ns)	α_3 (%)	$g^{(2)}(0)$
NQD1 (Fig. S3)	Before advancing	75	2.1	33.4	25.7	66.6	-	-	0.08
	10 nm	30	0.7	42.5	3.6	46.3	10.1	11.2	0.24
	6 nm	25	0.6	65.0	1.3	34.7	9.0	0.3	0.90
	2 nm	5	0.3	98.8	4.4	1.2	-	-	-
	After retracting	70	1.7	28.8	32.6	71.2	-	-	0.08
NQD2 (Fig. S4)	Before advancing	140	1.2	73.3	24.8	26.7	-	-	0.07
	10 nm	50	1.0	60.0	6.2	40.0	-	-	0.22
	6 nm	30	0.8	65.6	2.9	34.4	-	-	0.61
	2 nm	20	0.6	89.0	1.8	11.0	-	-	-
	After retracting	135	1.4	31.6	30.8	68.4	-	-	0.07

PL decay curves were fitted by a sum of two- or three-exponential functions, $I(t) = \alpha_1 exp(-t/\tau_1) + \alpha_2 exp(-t/\tau_2) + \alpha_2 exp(-t/\tau_3)$, where τ and α represent the PL lifetime and the normalized amplitude, respectively.

4-2. Excitation at 465 nm

Figures S5-S7 show the three representative emission behaviors of a single NQD with an approaching AgTip, as measured at 465 nm excitation. The PL intensity, PL lifetime, normalized amplitude, and the $g^{(2)}(0)$ value obtained from Figures S5-S7 are summarized in Table S2. The PL intensity increased with a shortening of the decay curves, and the probability of multiphoton emission increased with decreasing *z*-distance. After the AgTip was retracted, the emission behavior returned to the original emission behavior, similar to the emission behavior discussed in the main text. In the case of the single NQD shown in Figure S6, the enhancement of the $g^{(2)}(0)$ and the shortening of the decay curve were smaller compared with the other single NQDs, indicating that the interaction with the AgTip was weaker. We considered this result to be typical emission behavior caused by the deviation of the distance; i.e., the position of the AgTip was not perfectly consistent with the single NQD in the *xy* plane.

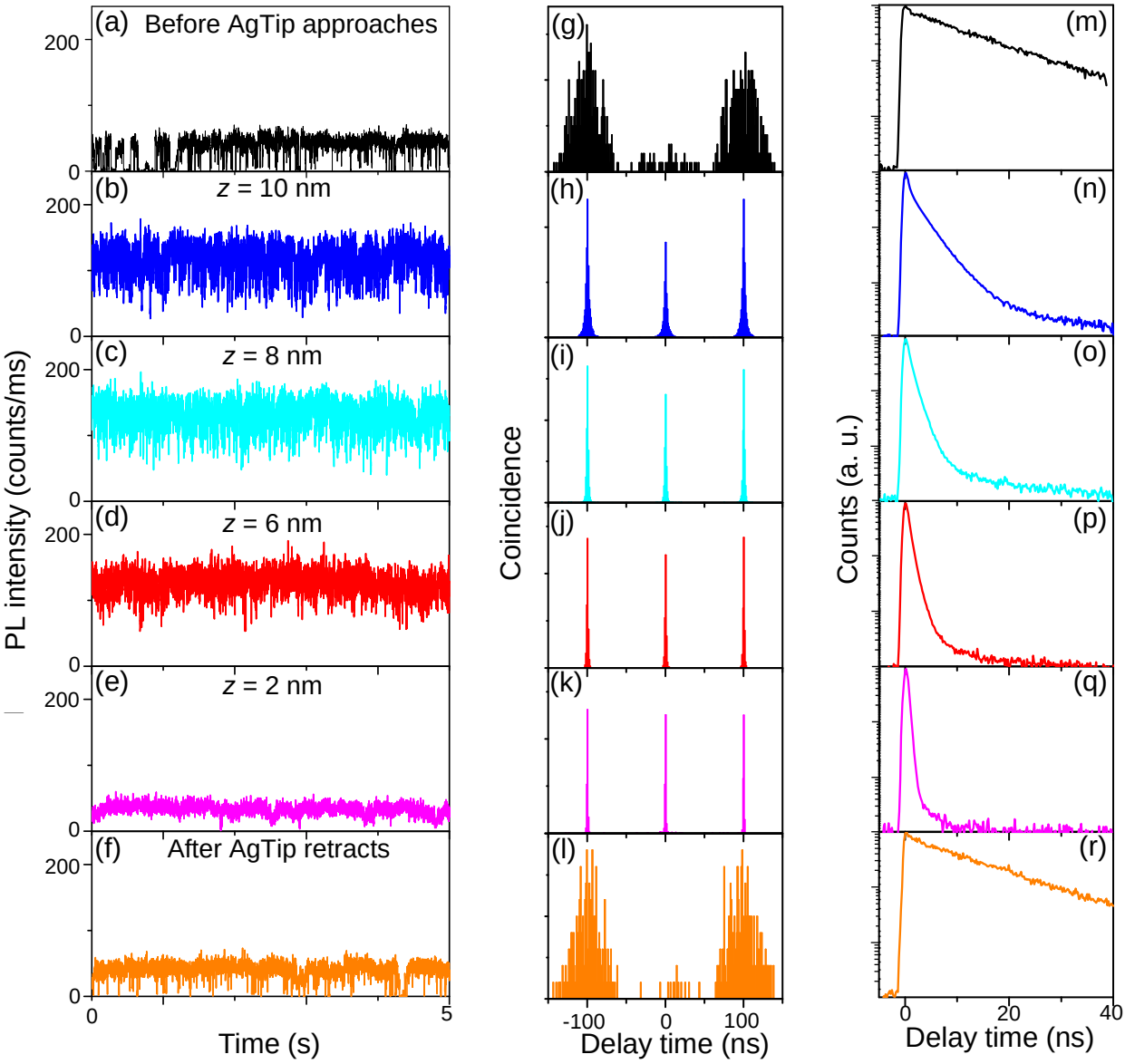

Figure S5. Time traces of the PL intensity (a-f), photon correlation histograms (g-l), and PL decay curves (m-r) detected from a single NQD depending on the *z*-distance; the excitation wavelength was 465 nm. (a, g, m) Before the AgTip was advanced; (b, h, n) z = 10 nm; (c, i, o) z = 8 nm; (d, j, p) z = 6 nm; (e, k, q) z = 2 nm; and (f, l, r) after the AgTip was retracted.

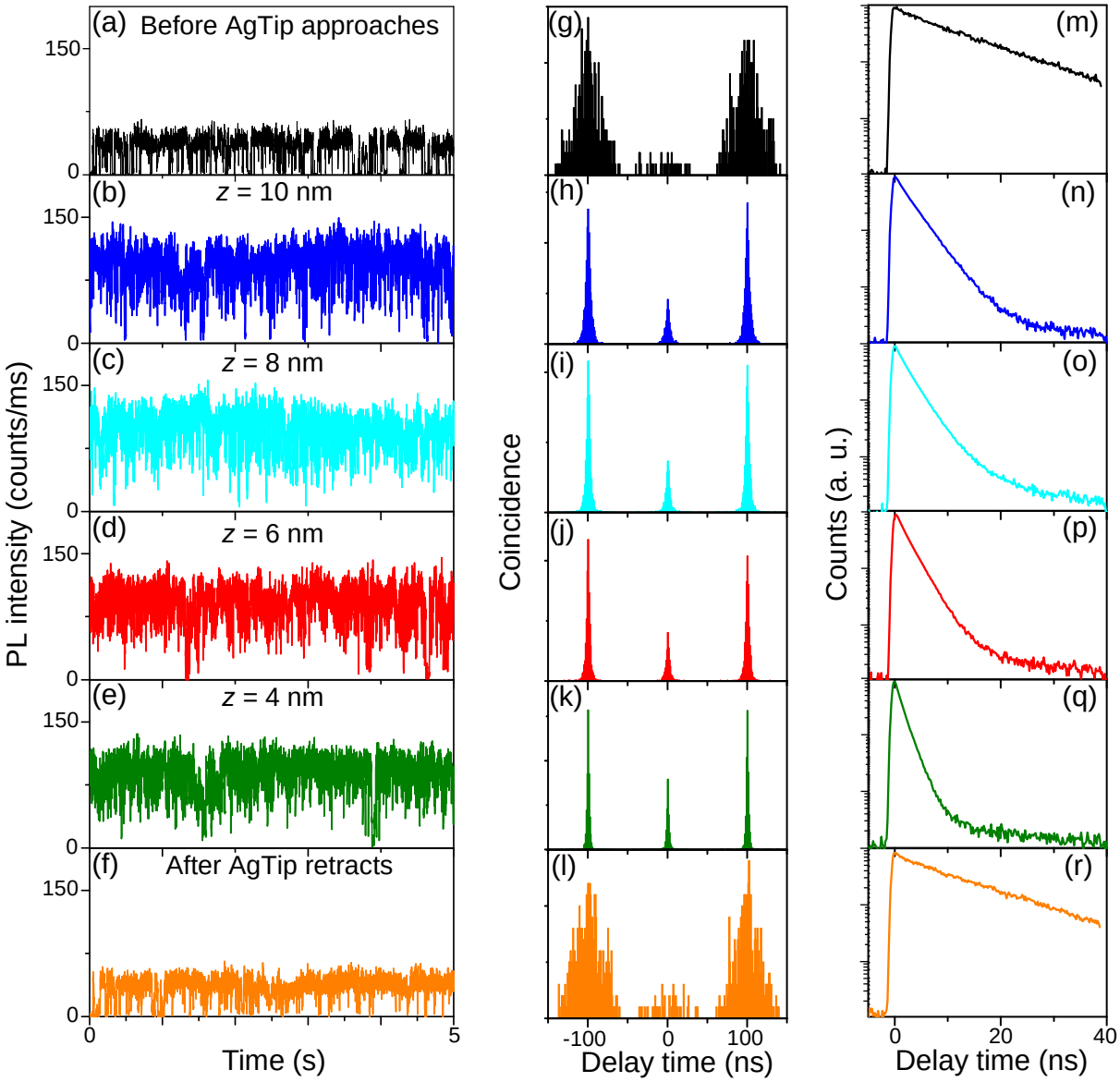

Figure S6. Time traces of the PL intensity (a-f), photon correlation histograms (g-l), and PL decay curves (m-r) detected from a single NQD depending on the *z*-distance; the excitation wavelength was 465 nm. (a, g, m) Before the AgTip was advanced; (b, h, n) z = 10 nm; (c, i, o) z = 8 nm; (d, j, p) z = 6 nm; (e, k, q) z = 4 nm; and (f, l, r) after the AgTip was retracted.

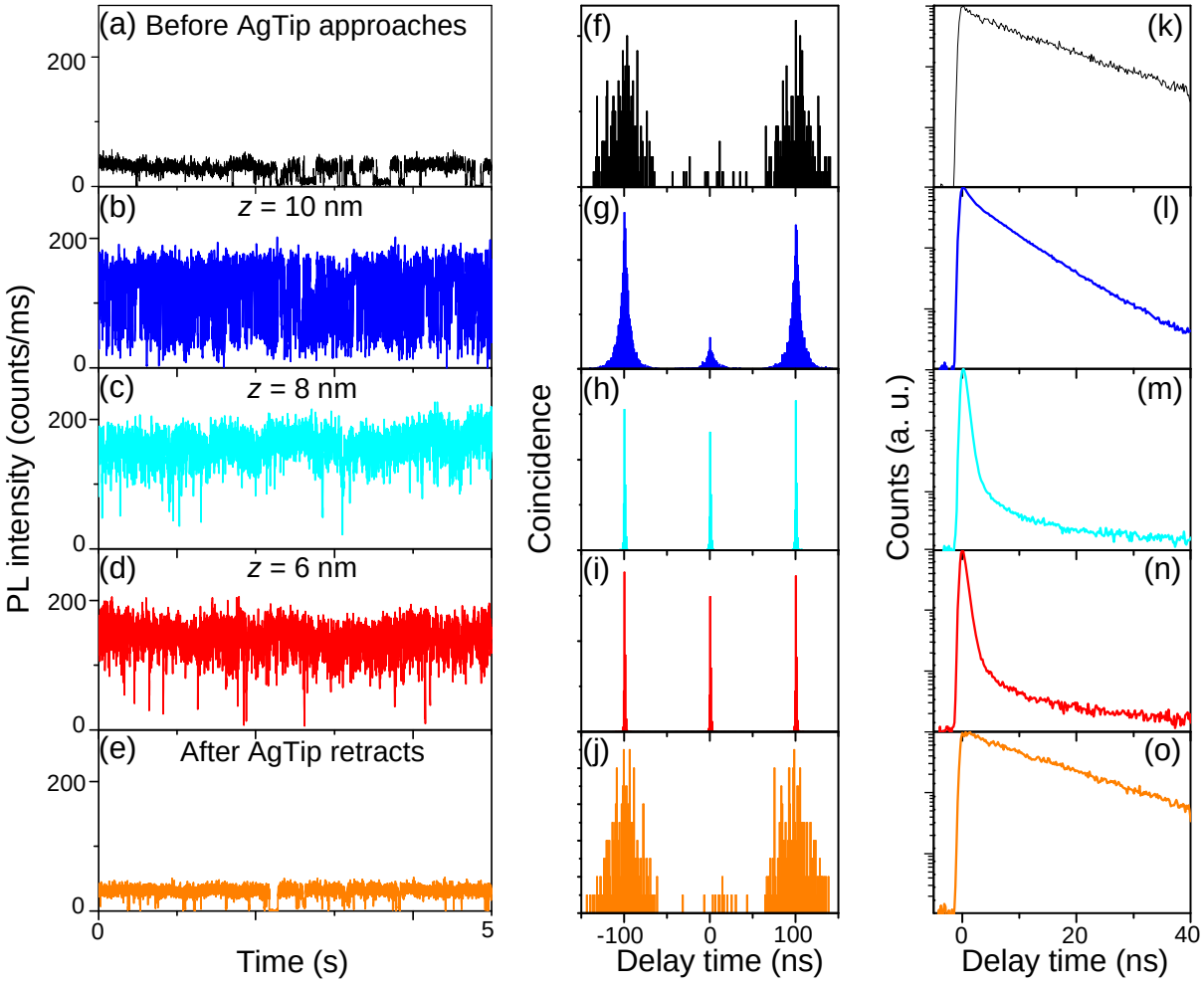

Figure S7. Time traces of the PL intensity (a-e), photon correlation histograms (f-j), and PL decay curves (k-o) detected from a single NQD depending on the *z*-distance; the excitation wavelength was 465 nm. (a, f, k) Before the AgTip was advanced; (b, g, l) z = 10 nm; (c, h, m) z = 8 nm; (d, i, n) z = 6 nm; and (e, j, o) after the AgTip was retracted.

Table S2. The PL intensity, fitting parameters for the PL decay curves, and $g^{(2)}(0)$ obtained from single NQDs shown in Figures S5-S7.

	z-distance	Intensity (cts/ms)	τ_1 (ns)	α_1 (%)	τ_2 (ns)	α_2 (%)	τ_3 (ns)	α_3 (%)	$g^{(2)}(0)$
NQD1 (Fig. S5)	Before advancing	60	0.6	7.7	33.3	92.3	-	-	0.13
	10 nm	170	0.4	52.9	2.3	44.8	5.2	2.3	0.63
	8 nm	180	0.4	62.5	1.1	37.3	6.5	0.2	0.77
	6 nm	160	0.4	77.1	0.9	22.8	4.7	0.1	0.84
	2 nm	40	0.3	99.8	3.1	0.2	-	-	1.00
	After retracting	60	29.9	100	-	-	-	-	0.08
NQD2 (Fig. S6)	Before advancing	60	3.6	8.3	28.4	91.7	-	-	0.10
	10 nm	145	0.8	11.2	2.9	88.2	9.6	0.6	0.30
	8 nm	145	0.8	16.0	2.4	82.0	6.9	2.0	0.36
	6 nm	140	0.8	17.0	2.1	82.6	8.1	0.4	0.36
	4 nm	130	0.8	56.7	1.4	43.2	9.4	0.1	0.50
	After retracting	60	2.3	7.9	28.1	92.1	-	-	0.12
NQD3 (Fig. S7)	Before advancing	50	1.6	9.4	29.7	90.6	-	-	0.07
	10 nm	180	1.1	38.4	5.6	58.3	11.6	3.3	0.16
	8 nm	200	0.4	99.3	2.3	0.6	10.7	0.1	0.84
	6 nm	180	0.4	98.9	2.2	1.0	10.6	0.1	0.87
	After retracting	50	30.2	100	-	-	-	-	0.05

References

1. Masuo, S.; Kanetaka, K.; Sato, R.; Teranishi, T. *ACS Photonics* **2016,** *3*, 109-116.

2. Maus, M.; Cotlet, M.; Hofkens, J.; Gensch, T.; De Schryver, F. C.; Schaffer, J.; Seidel, C. A. M. *Anal. Chem.* **2001,** *73*, 2078-2086.

3. Ren, F.; Takashima, H.; Tanaka, Y.; Fujiwara, H.; Sasaki, K. *Opt. Express* **2013,** *21*, 27759-27769.

4. Johnson, P. B.; Christy, R. W. *Phys. Rev. B* **1972,** *6*, 4370-4379.